

Dihydride dimer structures on the Si(100):H surface studied by low-temperature scanning tunneling microscopy

Amandine Bellec,* Damien Riedel, and Gérald Dujardin

Laboratoire de Physique Moléculaire, CNRS, Bat. 210, Université Paris Sud, 91405 Orsay, France

Nikolaos Rompotis and Lev N. Kantorovich

King's College London, Strand, London WC2R 2LS, United Kingdom

(Received 17 March 2008; revised manuscript received 13 June 2008; published 2 October 2008)

Surface reconstructions on the hydrogenated Si(100):H surface are observed and investigated by using a low-temperature (5 K) scanning tunneling microscope (STM). In addition to the well established 2×1 and 3×1 phases, linear structures extending over one to six silicon dimers along the same dimer row are observed. After a careful analysis of the corresponding STM topographies for both *n*-type and *p*-type doped silicon substrates, we conclude that these structures are dihydride dimers. This assignment is supported by *ab initio* density-functional calculations of the local density of states of dihydride structures of one or two dimers long. Furthermore, the calculation of the free-energy formation of our observed structure shows that their creation is closely linked with the hydrogenation process. These results demonstrate that the previous assignments of “split dimer” and “bow-tie” structures to dihydride dimers and dopant pairs, respectively, need to be reconsidered.

DOI: [10.1103/PhysRevB.78.165302](https://doi.org/10.1103/PhysRevB.78.165302)

PACS number(s): 68.47.Fg, 61.46.-w, 68.37.Ef

I. INTRODUCTION

The chemistry of hydrogen on the silicon (100) surface plays an important role for passivating silicon surfaces in microelectronic processing.¹⁻⁴ In the context of molecular electronics, hydrogenated silicon surfaces are also used for atomic-scale patterning of reactive sites^{5,6} or conducting lines.⁷⁻¹² As a result, the atomic structures of hydrogenated Si(100) surfaces have attracted much attention over the past few years.¹³⁻¹⁵ The adsorption of hydrogen atoms on the Si(100) surface can lead to different surface reconstructions, depending on the surface temperature during the hydrogen adsorption-desorption cycles.^{16,17} At a surface temperature of 650 K, a monolayer of adsorbed hydrogen produces mainly a 2×1 reconstruction [Fig. 1(a)]. A higher coverage of 1.33 monolayers can be obtained at a surface temperature of 400 K, corresponding to a 3×1 reconstruction [Fig. 1(b)]. At room temperature (300 K), it is possible to obtain a 1×1 reconstruction¹⁸⁻²¹ with a hydrogen coverage of two monolayers.

Among these reconstructions, Qin and Norton²² showed that the phase transition between 2×1 and 3×1 domains at 400 K can be strongly influenced by H₂ adsorption, leading to the formation of small 1×1 (dihydride) areas. Other silicon hydride structures called “split dimers” have been observed²³ on hydrogenated silicon surface prepared above 600 K. These split-dimer structures have been assigned to dihydride dimers,²³ although it is generally considered that dihydride structures are not stable at 600 K. Recently, Suwa *et al.*²⁴ observed different surface structures, called “bow-tie” structures, on the H-terminated Si(100)- 2×1 surface at 80 K, which they have assigned to dopant pairs segregated from the bulk material. These one-dimer length bow-tie structures have been observed to coexist with split-dimer structures.²⁴

In this paper we investigate thoroughly the various reconstructions of the hydrogenated Si(100) surface by using a

low-temperature (5 K) scanning tunneling microscope (LT-STM) and a room-temperature STM. In addition to the 2×1 and 3×1 phases coexisting with the previously bow-tie and split-dimer structures, we found structures that extend up to six silicon dimers along the same dimer row. Some of these structures having the size of a single silicon dimer are identical to those observed by Suwa *et al.*²⁴ After a careful analysis of the STM topographies and the length distribution of these structures for both *n*-type and *p*-type doped Si(100), we reassign the bow-tie structures to the formation of dihydride dimers, shown schematically in Fig. 1(c), rather than to the segregation of dopant pairs. Our assignment is supported by *ab initio* density-functional theory (DFT) calculations of the local density of states (LDOS) of these structures as well as their free energies of formation. In the light of these results, the previous assignment of the split dimer to dihydride dimers fails and alternative assignments are discussed.

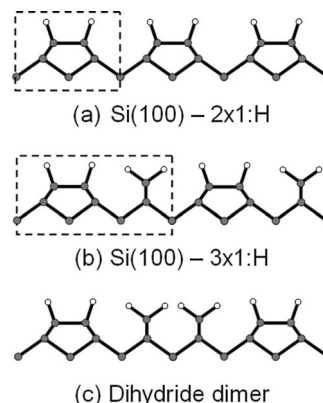


FIG. 1. Cross-sectional view of the different reconstructions observed on the Si(100):H surface. (a) Si(100)- 2×1 :H. (b) Si(100)- 3×1 :H. (c) Dihydride dimer (1×1). The dash rectangles indicate the unit cell of the two first reconstructions.

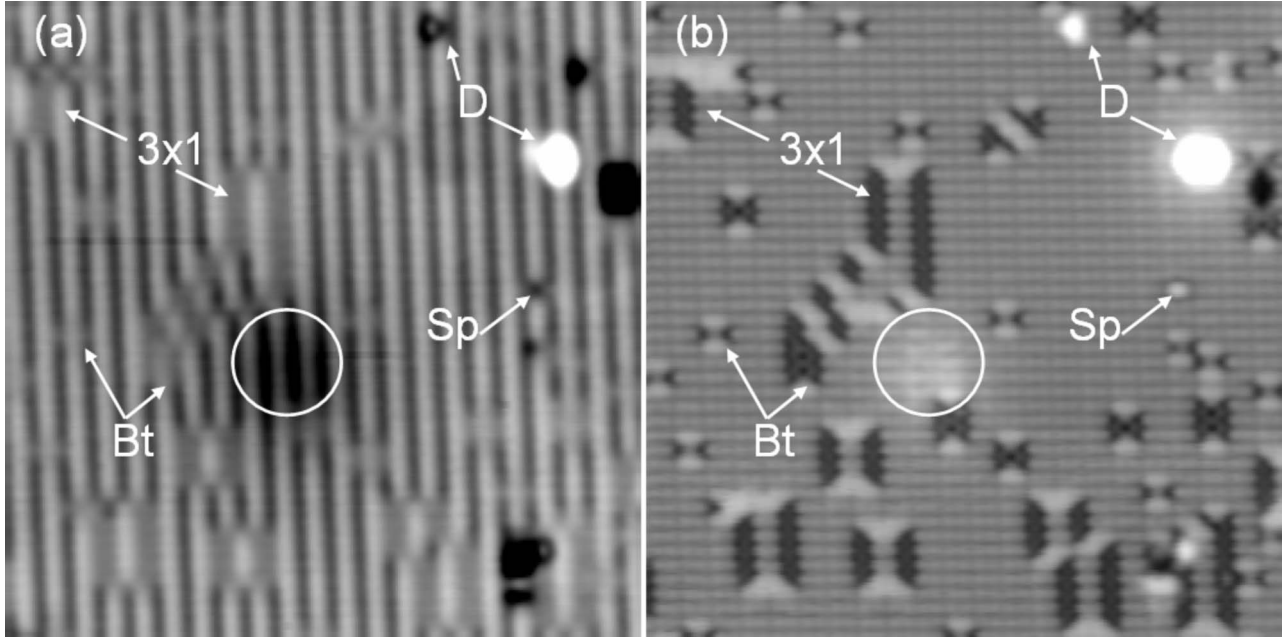


FIG. 2. $170 \times 170 \text{ \AA}^2$ STM topographies of a p -doped Si(100)- 2×1 :H surface at 5 K for (a) filled states ($V_S = -2.5 \text{ V}$ and $I = 110 \text{ pA}$) and (b) empty states ($V_S = 1.7 \text{ V}$ and $I = 110 \text{ pA}$). The Bt notation stands for the bow-tie structures, Sp for the split-dimer structures, and D for unknown defects. The white circle indicates the presence of a subsurface dopant.

II. EXPERIMENTS

Experiments are performed using a LT-STM (Createc) under ultrahigh-vacuum (UHV) conditions. Si(100) samples are As doped (n type), with a resistivity of $5 \text{ m}\Omega \text{ cm}$, and B doped (p type), with a resistivity of $6 \text{ m}\Omega \text{ cm}$. After preparing clean Si(100)- 2×1 surfaces under UHV (base pressure 1.10^{-10} Torr),²⁵ hydrogenation of the clean Si(100) surface is performed, as previously reported,^{16,26} with the sample kept at 650 K. After hydrogenation, the sample is cooled down and transferred to the STM chamber.

III. RESULTS AND DISCUSSION

Figure 2 shows STM topographies of the Si(100):H surface for both negative [Fig. 2(a)] and positive [Fig. 2(b)] sample biases. As expected from the experimental parameters used for the hydrogenation,^{16,26} the main reconstruction of the Si(100):H surface is the 2×1 reconstruction (see Fig. 2 and Table I). However, the 2×1 phase coexists with small areas of 3×1 reconstruction. As seen in Fig. 2, the rows of 3×1 unit cells (rectangles) always appear in pairs. This is in agreement with the phase transition between the 2×1 and

the 3×1 reconstruction, which is known to involve the adsorption of H_2 molecules, each producing a pair of 3×1 unit cells.²² Other structures can be observed in Fig. 2: bow-tie structures (Bt) that can extend up to six dimers. One can see that Bt structures that are made of a single dimer are completely similar to the structures observed by Suwa *et al.*²⁴ at 80 K in both empty and filled state STM topographies. A split dimer (Sp) is also observed in Fig. 2 with a characteristic empty state STM topography; the dark center part of the Sp dimer observed at negative sample bias [Fig. 2(a)] appears as a bright protrusion when the Sp dimer is observed at positive sample bias [Fig. 2(b)]. This Sp dimer STM topography is identical to what has been observed at room temperature^{23,27,28} and at 80 K.²⁴ Other features of Fig. 2, such as defects (D) or subsurface dopant induced features²⁹ (white circle), are not considered in this study.

A careful look at the Bt structures (circles in Fig. 3) when observed at negative sample bias [Fig. 3(a)] shows structures that are hardly distinguishable from the 2×1 reconstruction, except for a blurred contour of the corresponding 2×1 unit cells. This blurred contour surrounding the 3×1 and Bt structures at negative sample bias STM topographies is also very similar to what has been observed by Suwa *et al.*²⁴ at 80 K and is routinely observed at 5 K. However, at positive sample bias [Fig. 3(b)], one can easily see these structures whose lengths extend up to six silicon dimers along a dimer row. This observation points out that the Bt structures are often mixed with the 3×1 reconstruction as seen in the center of Fig. 3(b). Furthermore, the 3×1 reconstruction and the Bt structures have very similar STM topographies especially at negative sample bias. The Sp structure observed in Fig. 2 is different from the 3×1 and the Bt structures since it does not show this blurred contour [Fig. 2(b)].

TABLE I. Proportion of each type of dimer reconstruction observed on the Si(100):H surface.

Sample	2×1	3×1	bow-tie	other
n type (As doped)	$66.8 \pm 0.5\%$	$23.0 \pm 0.5\%$	$5.3 \pm 0.2\%$	$4.9 \pm 0.2\%$
p type (B doped)	$79.8 \pm 0.3\%$	$9.3 \pm 0.2\%$	$3.9 \pm 0.2\%$	$7.0 \pm 0.2\%$

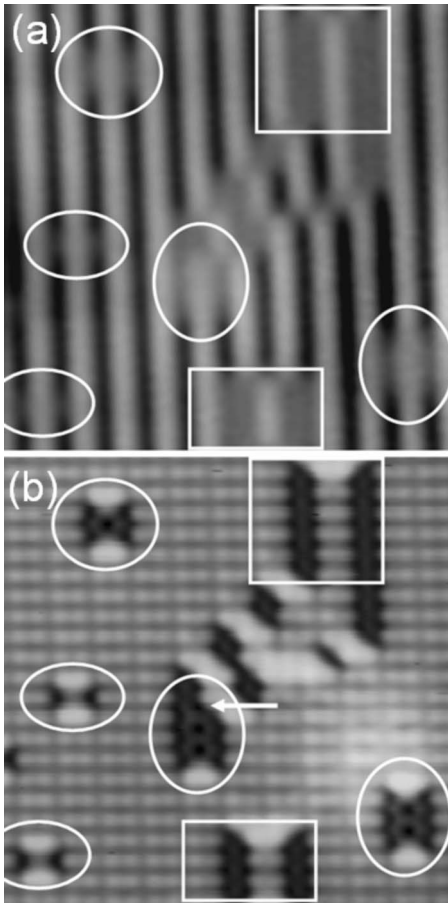


FIG. 3. STM topographies of the *p*-type Si(100):H surface ($83 \times 83 \text{ \AA}^2$) (a) sample bias $V_S = -2.5 \text{ V}$ and tunnel current $I = 110 \text{ pA}$, and (b) sample bias $V_S = 1.7 \text{ V}$ and tunnel current $I = 110 \text{ pA}$. Rectangles and circles show, respectively, the 3×1 and the dihydride dimer reconstructions.

As it will be discussed below, we assign the Bt structures to dihydride dimers rather than to the segregation of dopant pairs as suggested in Ref. 24. Understanding the previous assignments referring to dihydride dimers that have been previously proposed in the literature is a puzzling problem. Therefore a brief chronological summary is necessary. First, hydride dimers assigned as “antiphase boundaries composed of adjacent dihydride units” were observed at room temperature on the Si(100):H- 3×1 surface prepared at 400 K.²¹ Their unoccupied state STM topographies can be described as long features extending over more than ten silicon dimers. Second, small rows of dihydride dimers were also observed at room temperature as a result of the phase transition between the 2×1 and 3×1 reconstructions.²² However the low resolution unoccupied state STM topographies of this work does not allow a clear comparison to Bt or Sp structures. These authors refer to the work of Boland²¹ to describe their structures. Finally, isolated structures, called split dimers (Sp),^{23,27,28} have been assigned to dihydride dimers since almost 15 years ago, albeit without any real proof of it. Although this assignment was based on a vague resemblance with the 3×1 unit cells STM topographies, only filled state STM topographies were considered.²³ Based on our observa-

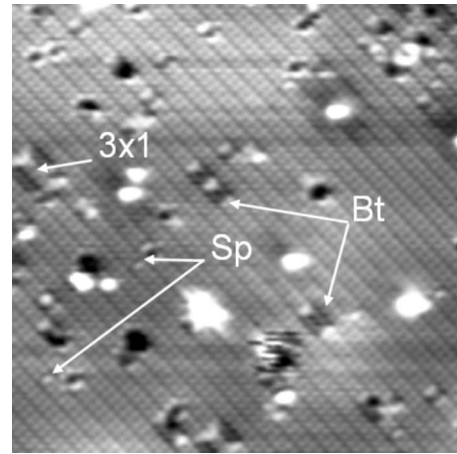


FIG. 4. $140 \times 140 \text{ \AA}^2$ STM empty state topography of a *n*-type Si(100)- 2×1 :H surface acquired at room temperature ($V_S = +2 \text{ V}$ and $I = 200 \text{ pA}$).

tion and model, we believe that these Sp structures have been incorrectly assigned to dihydride dimers.

One of the main arguments in favor of assigning the Bt structures to dihydride dimers is the observed mixture of bow-tie and 3×1 structures. This is seen in the central part of Fig. 3(b) (see arrow) where the structure continuously evolves from the bow-tie structure (below the arrow) to the 3×1 structure (above the arrow). Furthermore, the dark part of the 3×1 structure, which is known to be a dihydride silicon atom, has exactly the same appearance in the STM topography as each half of the bow-tie structure. This is not the case for Sp dimers since their empty state STM topography [Fig. 2(b)] shows a bright feature centered on its dimer. Moreover, the Bt structures, whatever their length, have other similar features with the 3×1 reconstruction areas. For example, the monohydride dimers at each end appear brighter in the unoccupied state STM topography [Fig. 3(b)]. These observations favor our proposed reassignment of dihydride dimer structures [Fig. 1(c)] to the Bt structures.

We emphasize that Sp dimers have been observed at room temperature,^{23,27,28} at 80 K,²⁴ and in the present work at 5 K. To verify whether the Bt structures observed at 80 (Ref. 24) and 5 K (present work) can be observed at 300 K, we have performed a hydrogenation of the same type of silicon substrate at 650 K and recorded the surface topography with a room-temperature STM. The result shown in Fig. 4 reveals that both Bt and Sp structures can be observed together with 3×1 reconstruction areas. Therefore, the substrate temperature cannot account for specific observations of the dihydride structures, and the formation of long Bt structures is observed at both room temperature and 5 K.

To further confirm that Bt structures are dihydride dimers, we have performed a local desorption of the hydrogen atoms of a Bt structure observed at 5 K. To perform this manipulation, the STM tip is positioned on top of the Bt structure (blue circle in Fig. 5), then we applied a surface voltage pulse at $V_S = +2.5 \text{ V}$ during 2 s. When reimaging the same area [Fig. 5(b)], a bright feature formed by two parallel lobes is observed at the position of the Bt structure. This feature is similar to the one produced by the same surface voltage

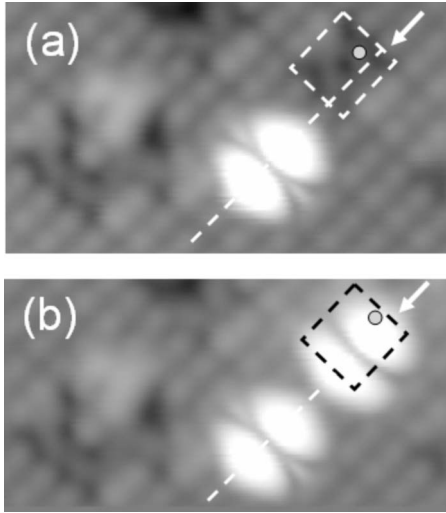


FIG. 5. STM topographies of a *p*-type Si(100)-2×1:H surface acquired at 5 K. (a) 53×29 Å², empty states, ($V_S=+1.7$ V and $I=250$ pA). (b) Same as (a) after a surface voltage pulse (on the blue circle) at $V_S=+2.5$ V during 2 s. The dotted line indicates the position of the dehydrogenated dimers. The dotted square indicates the position of the two dimers Bt structure.

pulse beside the Bt structure on a nearby monohydride dimer and is characteristic of the empty state STM topography of a single dehydrogenated dimer.³⁰ The dotted line drawn in Fig. 5 crossing both dehydrogenated dimers indicates at which position inside the Bt structure the desorption has occurred. This result confirms the hydrogenated nature of Bt structures and further proves that they cannot be assigned as dopant pair segregation.²⁴ Indeed, if a two-dimer-long Bt structure was made of hydrogenated phosphorous dimers similar to what is described by Suwa *et al.*, a single dehydrogenated phosphorous dimer would not be identical to the dehydrogenated silicon dimer observed in Fig. 5(b). This is because the formed phosphorous dimer would have no dangling bond.

Table I presents the proportion of each type of reconstruction (2×1, 3×1, and Bt) on the Si(100):H surface for *n*-type (As-doped) and *p*-type (B-doped) samples at 5 K. Surprisingly, Sp dimers are very rarely observed (<1%) on the surface and always are on a single dimer compared to the other structures. Within experimental uncertainties, both types of samples show almost similar proportions of bow-tie structures. It is therefore very unlikely that these structures are due to the surface segregation of dopant atoms since the surface segregation of boron dopant atoms is energetically unfavorable.^{24,29,31}

To support our assignment of Bt structures to dihydride dimers [Fig. 1(c)], we have simulated STM images of these dihydride dimer structures using the Tersoff-Hamman approximation.³² We used the plane-wave VASP code,^{33,34} which implements periodic boundary conditions, generalized gradient approximation (GGA) density functional,³⁵ and the method of ultrasoft pseudopotentials.³⁶ The chosen simulated cell in each case depends on the bow-tie structure size and is sufficiently big to avoid interactions between periodically repeated images. For a Bt structure of *N* dimers, the cell size is 3(*N*+1). Thus, only a single **k**=0 point was used in relax-

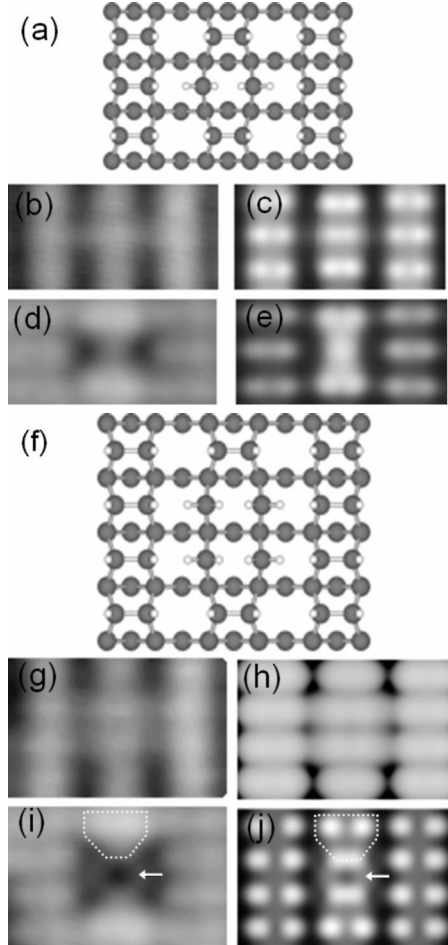


FIG. 6. Experimental topographies [(b), (d), (g), and (i)] and calculated LDOS [(c), (e), (h), and (j)] for one [(a)–(e)] and two-dimer [(f)–(j)] dihydride structures. The upper three atomic layers of the corresponding relaxed structures are shown in (a) and (f). [(b) and (g)] STM topographies of the *n*-type surface at $V_S=-1.7$ V and $I=69$ pA. [(c) and (h)] Calculated LDOS at negative bias (10^{-8} states/eV, integration performed from Fermi level to 1.2 eV). [(d) and (i)] STM topographies (*n*-type surface) at $V_S=1.7$ V and $I=69$ pA. [(e) and (j)] Calculated LDOS at positive bias (10^{-5} states/eV, integration performed from Fermi level to 1 eV).

ation calculations. Atomic positions were relaxed until the forces on atoms were less than 0.01 eV/Å. Among the different geometries tried, the most stable has symmetric Si-H bonds [Figs. 6(a) and 6(f)]. In Fig. 6 the experimental STM topographies of Bt structures are compared with the calculated LDOS (using several **k** points) for dihydride dimer structures composed of a single and two dimers, respectively. At both negative and positive sample biases, the simulations are in reasonable agreement with the experimental STM topographies. The blurred features of the Bt structures observed in filled state topographies are particularly well reproduced for both the one-dimer [Fig. 6(c)] and two-dimer [Fig. 6(h)] structures. For the one-dimer structures, the simulated dihydride dimer and the two neighbor monohydride dimers that end the Bt structure along the same dimer row appear brighter than the other monohydride dimers [see Figs. 6(d), 6(e), and 2(a)]. None of the one-dimer Sp structures are ob-

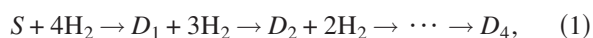
TABLE II. Measured and calculated (within the random model) probabilities of the three possible configurations around a bow-tie dimer. 1 symbolizes a bow-tie dimer and 0 a monohydride dimer, while p is the proportion of bow-tie dimers on the surface.

Sample	Case	Measured	Model	Calculated
n type	010	$37.4 \pm 3.2\%$	$(1-p)^2$	89.7%
	011 or 110	$47.7 \pm 3.4\%$	$2p(1-p)$	10.0%
	111	$14.9 \pm 2.4\%$	p^2	0.3%
p type	010	$47.9 \pm 2.7\%$	$(1-p)^2$	92.1%
	011 or 110	$40.8 \pm 2.7\%$	$2p(1-p)$	7.7%
	111	$11.3 \pm 1.7\%$	p^2	0.2%

served experimentally perturbing the surrounding monohydride dimers in the same way although they appear as bright features as well [see Fig. 2(b)]. For the two-dimer Bt structure, the bright features that end the Bt structures are also depicted [see the dotted lines in Figs. 6(i) and 6(j)] as well as the dark central part of the two-dimer Bt structure [see arrows in Figs. 6(i) and 6(j)] whose position is characteristically located in between the adjacent monohydride silicon dimers [see Figs. 2(b) and 3(b)].

To understand how the bow-tie structures are formed, we calculate the probabilities of finding various configurations of dimers around a chosen dihydride dimer, assuming a completely random distribution of dihydride dimers in the dimer row. Each Bt dimer is considered as an ‘‘occupied’’ site denoted by 1, while the monohydride dimers are considered as ‘‘unoccupied’’ sites denoted by 0. Since there are two nearest neighbors along a dimer row, three cases are possible: (i) both neighbor sites of the given dihydride dimer are unoccupied (configuration 010), (ii) only one site is occupied (configurations 110 and 011), and (iii) both sites are occupied (111).³⁷

The comparison between experimental distribution of the Bt structure and calculated probabilities for the three cases (Table II) clearly shows that the distribution of the Bt dimers is not purely random: the measured distribution of two Bt dimers side by side (011, 110, and 111) is more than 50% for both n - and p -type surfaces, whereas the random model predicts only 10%. This means that there is some interaction between the Bt dimers during the formation of longer structures, suggesting that, during the surface hydrogenation, a Bt structure is able to stimulate the dissociative adsorption of an H_2 molecule on one of the adjacent monohydride dimers or the clustering with other dihydride dimers migrating across the surface. If the observed Bt structures were to be assigned to the surface segregation of pairs of dopant atoms, it would be necessary to assume attractive interactions between dopant pairs, which are very unlikely to occur. The preferential formation of dihydride dimers close to existing ones is confirmed by our *ab initio* DFT calculations of their free energies of formation corresponding to the chain of reactions:



where D_n is the structure containing n adjacent dihydride dimers along the same dimer row and S stands for the surface

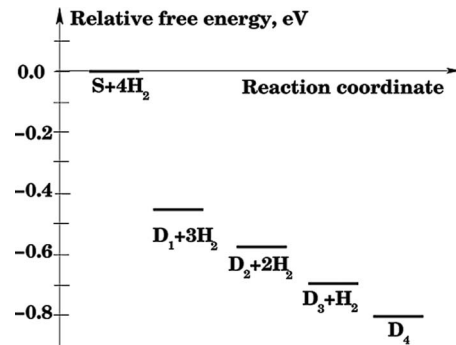


FIG. 7. Calculated relative free energies of four dihydride dimer systems D_1, \dots, D_4 corresponding to the chain reaction (1) of the H_2 molecule attachment (see text). Note that the barriers have not been calculated.

containing only monohydride dimers. The free energy of each system is obtained by adding the zero-phonon energy to the total DFT energy of the relaxed system. The phonon frequencies are obtained numerically using the TETR code³⁸ by calculating changes in forces due to small atomic displacements. Figure 7 shows the calculated relative free energies for D_n systems containing up to four dihydride dimers ($n=1-4$) corresponding to the reactions (1). The energy change due to the formation of the first dihydride dimer on a surface containing only monohydride dimers (about 0.45 eV) differs significantly from the energy differences (around 0.1 eV) corresponding to the formation of every consecutive dihydride dimer. Adding a H_2 molecule to the existing D_1 system to form two consecutive dihydride dimers (D_2) lowers the surface energy by 0.12 eV; adding the third and the fourth H_2 molecules to form D_3 and D_4 systems lowers the system energy by 0.13 and 0.1 eV, respectively. This result demonstrates that the clustering of dihydride dimers along the same dimer row is found to be energetically favorable; thus the formation of elongated dihydride systems is not at all random. This suggests that the formation of dihydride dimers, observed as Bt structures along the same row, may contribute to the growth of 3×1 structure in competition with other suggested mechanisms.²²

Both Sp and Bt structures are observed at room temperature, at 80 K and at 5 K. As Sp and Bt structures have markedly different STM topographies, the assignment of Bt structures to dihydride dimers clearly prevents assigning of Sp dimers to the same dihydride dimer structures. Many other structures may account for the observation of Sp structures. It is beyond the scope of this paper to depict in details the Sp structure. However, we may formulate some suggestions. One possibility could be a partial hydrogenation of a silicon dimer such as a Si_2H_3 structure where one H atom bridges two Si atoms. Nevertheless, it is hardly possible that such a structure is stable, especially during preparations of the surface at 650 K. Another structure that can be envisaged is a Si_2H_2O dimer where, this time, the oxygen atom bridges two Si atoms. This structure might be more stable than the first one and can be favored by the residual water present in the vacuum chamber during the hydrogenation process. Besides, the STM topographies of siloxane dimers have strong similarities with the observed Sp structure.³⁹⁻⁴¹

IV. CONCLUSION

In conclusion, low-temperature STM topographies of the hydrogenated Si(100) surface show, in addition to the 2×1 and 3×1 reconstructions, bow-tie structures whose length (n) can extend from one to six silicon dimers. Similar structures with $n=1$ have been previously assigned to the segregation of dopant pairs.²⁴ The present results do not support this assignment. High resolution STM topographies recorded at both negative and positive sample biases show similarities between the bow-tie structures and the dihydride part of the 3×1 structures, as well as the continuous topographic evolution between the bow-tie and 3×1 structures. This leads us to assign the bow-tie structures to dihydride dimers. This is

further confirmed by comparing n -type (As-doped) and p -type (B -doped) silicon samples, as well as experimental STM topographies with calculated densities of states. Finally, the experimentally observed clustering of the bow-tie structures is well explained by the free-energy calculation of the formation of dihydride dimer rows. Therefore, it appears that the split dimers should not be ascribed to dihydride dimers.

ACKNOWLEDGMENT

This work is supported by the European Integrated project PicoInside (Contract No. FGP-015847).

*amandine.bellec@u-psud.fr

- ¹J. W. Lyding *et al.*, Appl. Surf. Sci. **132**, 221 (1998).
- ²M. C. Hersam, N. P. Guisinger, J. Lee, K. G. Cheng, and J. W. Lyding, Appl. Phys. Lett. **80**, 201 (2002).
- ³C. P. Herrero, M. Stutzmann, and A. Breitschwerdt, Phys. Rev. B **43**, 1555 (1991).
- ⁴D. Riedel, A. J. Mayne, and G. Dujardin, Phys. Rev. B **72**, 233304 (2005).
- ⁵M. C. Hersam, N. P. Guisinger, and J. W. Lyding, Nanotechnology **11**, 70 (2000).
- ⁶A. J. Mayne, L. Soukiassian, N. Commaux, G. Comtet, and G. Dujardin, Appl. Phys. Lett. **85**, 5379 (2004).
- ⁷E. T. Foley, A. F. Kam, J. W. Lyding, and P. Avouris, Phys. Rev. Lett. **80**, 1336 (1998).
- ⁸K. Kato, H. Kajiyama, S. Heike, T. Hashizume, and T. Uda, Phys. Rev. Lett. **86**, 2842 (2001).
- ⁹T. Hitosugi, S. Heike, T. Onogi, T. Hashizume, S. Watanabe, Z. Q. Li, K. Ohno, Y. Kawazoe, T. Hasegawa, and K. Kitazawa, Phys. Rev. Lett. **82**, 4034 (1999).
- ¹⁰M. Sakurai, C. Thirstrup, and M. Aono, Phys. Rev. B **62**, 16167 (2000).
- ¹¹P. Doumergue, L. Pizzagalli, C. Joachim, A. Altibelli, and A. Baratoff, Phys. Rev. B **59**, 15910 (1999).
- ¹²L. Soukiassian, A. J. Mayne, M. Carbone, and G. Dujardin, Surf. Sci. **528**, 121 (2003).
- ¹³S. Ciraci, R. Butz, E. M. Oellig, and H. Wagner, Phys. Rev. B **30**, 711 (1984).
- ¹⁴J. E. Northrup, Phys. Rev. B **44**, 1419 (1991).
- ¹⁵P. G. Piva, G. A. DiLabio, J. L. Pitters, J. Zikovskiy, M. Rezeq, S. Dogel, W. A. Hofer, and R. A. Wolkow, Nature (London) **435**, 658 (2005).
- ¹⁶J. J. Boland, Adv. Phys. **42**, 129 (1993).
- ¹⁷K. W. Kolasinski, W. Nessler, A. de Meijere, and E. Hasselbrink, Phys. Rev. Lett. **72**, 1356 (1994).
- ¹⁸T. Sakurai and H. D. Hagstrum, Phys. Rev. B **14**, 1593 (1976).
- ¹⁹S. Maruno, H. Iwasaki, K. Horioka, S.-T. Li, and S. Nakamura, Phys. Rev. B **27**, 4110 (1983).
- ²⁰K. Oura, J. Yamane, K. Umezawa, M. Naitoh, F. Shoji, and T. Hanawa, Phys. Rev. B **41**, 1200 (1990).
- ²¹J. J. Boland, Surf. Sci. **261**, 17 (1992).
- ²²X. R. Qin and P. R. Norton, Phys. Rev. B **53**, 11100 (1996).
- ²³E. J. Buehler and J. J. Boland, Surf. Sci. **425**, L363 (1999).
- ²⁴Y. Suwa, S. Matsuura, M. Fujimori, S. Heike, T. Onogi, H. Kajiyama, T. Hitosugi, K. Kitazawa, T. Uda, and T. Hashizume, Phys. Rev. Lett. **90**, 156101 (2003).
- ²⁵D. Riedel, M. Lastapis, M. G. Martin, and G. Dujardin, Phys. Rev. B **69**, 121301(R) (2004).
- ²⁶A. J. Mayne, D. Riedel, G. Comtet, and G. Dujardin, Prog. Surf. Sci. **81**, 1 (2006).
- ²⁷M. Fujimori, S. Heike, Y. Suwa, and T. Hashizume, Jpn. J. Appl. Phys., Part 2 **42**, L1387 (2003).
- ²⁸J. L. O'Brien, S. R. Schofield, M. Y. Simmons, R. G. Clark, A. S. Dzurak, N. J. Curson, B. E. Kane, N. S. McAlpine, M. E. Hawley, and G. W. Brown, Phys. Rev. B **64**, 161401(R) (2001).
- ²⁹L. Q. Liu, J. X. Yu, and J. W. Lyding, IEEE Trans. Nanotechnol. **1**, 176 (2002).
- ³⁰J. J. Boland, Phys. Rev. Lett. **67**, 1539 (1991).
- ³¹M. Ramamoorthy, E. L. Briggs, and J. Bernholc, Phys. Rev. Lett. **81**, 1642 (1998).
- ³²J. Tersoff and D. R. Hamann, Phys. Rev. B **31**, 805 (1985).
- ³³G. Kresse and J. Furthmüller, Comput. Mater. Sci. **6**, 15 (1996).
- ³⁴G. Kresse and J. Furthmüller, Phys. Rev. B **54**, 11169 (1996).
- ³⁵J. P. Perdew and Y. Wang, Phys. Rev. B **45**, 13244 (1992).
- ³⁶D. Vanderbilt, Phys. Rev. B **41**, 7892 (1990).
- ³⁷A. J. Mayne, C. M. Goringe, C. W. Smith, and G. A. D. Briggs, Surf. Sci. **348**, 209 (1996).
- ³⁸L. N. Kantorovich (www.cmmmp.ucl.ac.uk/~lev/codes/lev00).
- ³⁹A. Hemeryck, A. J. Mayne, N. Richard, A. Estève, Y. J. Chabal, M. D. Rouhani, G. Dujardin, and G. Comtet, J. Chem. Phys. **126**, 114707 (2007).
- ⁴⁰T. Uchiyama and M. Tsukada, Phys. Rev. B **55**, 9356 (1997).
- ⁴¹S.-Y. Yu, H. Kim, and J.-Y. Koo, Phys. Rev. Lett. **100**, 036107 (2008).